Mössbauer Study of the MoFe Protein of Nitrogenase from *Azotobacter vinelandii* Using Selective ^{57}Fe Enrichment of the M-Centers

Sun Jae Yoo,[†] Hayley C. Angove,[‡] Vasilios Papaefthymiou,[§] Barbara K. Burgess,[‡] and Eckard Münck*,[†]

Contribution from the Department of Chemistry, Carnegie Mellon University, Pittsburgh, Pennsylvania 15213, Department of Molecular Biology and Biochemistry, University of California, Irvine, California 92697-3900, and Department of Physics, Ioannina University, Ioannina, Greece

Received January 24, 2000

Abstract: The molybdenum−iron (MoFe) protein of nitrogenase contains two unique metalloclusters called P-cluster [8Fe-7S] and M-center (FeMo cofactor, [7Fe-9S-Mo-homocitrate]). Using samples containing M-centers selectively enriched with ^{57}Fe (^{57}M^{56}P), we have studied three M-center states with Mössbauer spectroscopy. The results are as follows. A detailed analysis of the Mössbauer spectra of the $S = {}^3/_2$ state M^N recorded in applied fields up to 8.0 T has revealed the features of the seventh Fe site which had eluded previous Mössbauer and ENDOR studies. This site has unusually small and anisotropic magnetic hyperfine interactions ($A_{iso} \approx -4$ MHz). Our studies have also revealed that the spectroscopic component previously labeled B^1 represents two equivalent Fe sites. Six of the M-center irons are trigonally coordinated to bridging sulfides; their unusual isomer shifts are discussed with particular reference to a trigonally coordinated Fe(II) thiolate complex synthesized by Power and co-workers (*Inorg. Chem.* **1995**, *34*, 1815−1822). The unusually low isomer shifts ($\delta_{av} = 0.41$ mm/s) of M^N suggest that the core of the M-center is (formally) best described as (Mo^{4+}-$3Fe^{3+}$-$4Fe^{2+}$). The turnover complex M^R is one electron further reduced than M^N. While δ_{av} changes by 0.06 mm/s between the one-electron oxidized state M^{OX} and M^N, only a small change in δ_{av}, 0.02 mm/s, is observed between M^N and M^R. Moreover, spectra of the integer-spin state M^R taken in strong applied magnetic fields are quite similar to those observed for M^N, suggesting that the 7-Fe segment of the M-center has the same spin structure in both states. These observations suggest that the reduction M$^N \rightarrow$ M^R is associated mainly with the molybdenum site. In a preliminary experiment, we have also observed reduction of the M-cluster (ca. 40%) by irradiating a ^{57}M^{56}P sample at 77 K in a synchrotron X-ray beam. The radiolytically reduced state, M^I, has integer electronic spin $S \geq 1$, and its reduction appears to be centered on the iron components of the cluster.

Introduction

Nitrogenase is composed of two separately purified proteins, the iron protein (Fe protein) and the molybdenum−iron protein (MoFe protein).[1] The Fe protein contains a single [4Fe-4S] cluster and serves as a very specific electron donor to the MoFe protein in a reaction that is somehow coupled to MgATP hydrolysis. The MoFe protein is an $\alpha_2\beta_2$ tetramer that contains two unique types of metal clusters. The [8Fe-7S] P-clusters appear to accept electrons from the Fe protein and transfer them to the [Mo-7Fe-9S-homocitrate] clusters that serve as the actual sites of dinitrogen binding and reduction.[1−4] When bound to the MoFe protein, the latter cluster-type was originally designated the M-center,[5] and this nomenclature will be used herein. More recently it has been referred to as the iron−molybdenum cofactor (FeMoco), a cluster that can also be isolated from the MoFe protein and studied as an independent entity in *N*-methyl formamide.[6,7]

X-ray crystallographic studies of MoFe proteins isolated from *Azotobacter vinelandii* (*Av*1),[8,9] *Clostridium pasteurianum* (*Cp*1),[10] and *Klebsiella pneumoniae* (*Kp*1)[11] have revealed that the M-center consists of two cuboidal fragments, [Mo-3Fe-3S] and [4Fe-3S], that are linked by three sulfide bridges (see Chart 1) and attached to the protein via two ligands. The sulfur of αCys275 coordinates to one of the irons of the [4Fe-3S] cubane to complete a tetrahedral coordination at Fe1. The pseudooctahedral coordination sphere of the Mo atom is completed by two oxygens supplied by the endogenous organic component homocitrate and by αHis442. An X-ray structure of isolated FeMoco is still not available.

* To whom correspondence should be addressed. Tel.: (412) 268-5058. Fax: (412) 268-1061. E-mail: em40@andrew.cmu.edu.
[†] Carnegie Mellon University.
[‡] University of California, Irvine.
[§] Ioannina University.

(1) Burgess, B. K.; Lowe, D. J. *Chem. Rev.* **1996**, *96*, 2983−3012.
(2) Smith, B. E.; Eady, R. R. *Eur. J. Biochem.* **1992**, *205*, 1−15.
(3) Seefeldt, L. C.; Dean, D. R. *Acc. Chem. Res.* **1997**, *30*, 260−266.
(4) Howard, J. B.; Rees, D. C. *Chem. Rev.* **1996**, *96*, 2965−2982.
(5) Münck, E.; Rhodes, H.; Orme-Johnson, W. H.; Davis, L. C.; Brill, W. J.; Shah, V. K. *Biochim. Biophys. Acta* **1975**, *400*, 32−53.
(6) Shah, V. K.; Brill, W. J. *Proc. Natl. Acad. Sci. U.S.A.* **1977**, *74*, 3249−3253.
(7) Burgess, B. K. *Chem. Rev.* **1990**, *90*, 1377−1406.
(8) (a) Chan, M. K.; Kim, J.; Rees, D. C. *Science* **1993**, *260*, 792−794. (b) Kim, J. Rees, D. C. *Science* **1992**, *257*, 1677−1682. (c) Kim, J.; Rees, D. C. *Nature* **1992**, *360*, 553−560.
(9) Peters, J. W.; Stowell, M. H. B.; Soltis, S. M.; Finnegan, M. G.; Johnson, M. K.; Rees, D. C. *Biochemistry* **1997**, *36*, 1181−1187.
(10) Kim, J.; Woo, D.; Rees, D. C. *Biochemistry* **1993**, *32*, 7104−7115.
(11) Mayer, S. M.; Lawson, D. M.; Gormal, C. A.; Roe, S. M.; Smith, B. E. *J. Mol. Biol.* **1999**, *292*, 871−891.

10.1021/ja000254k CCC: $19.00
Published on Web 05/06/2000

Chart 1

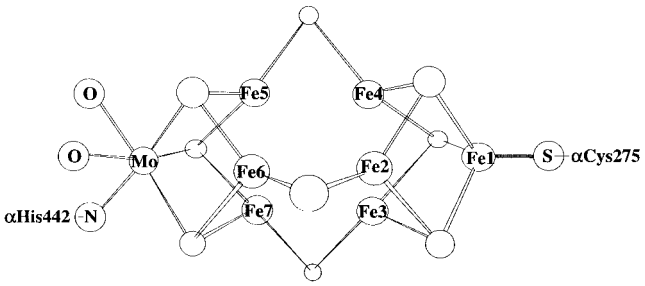

When the MoFe protein is isolated in the presence of excess dithionite, the M-center is in the oxidation state M^N ($S = {}^3/_2$) that yields a prominent EPR signal at $g = 4.32$, 3.68, and 2.01. The EPR signal exhibited by isolated FeMoco in NMF is similar to, although much broader than, the signal exhibited by the M-center of the MoFe protein, and both signals are unique in biology.[12−14] The $S = {}^3/_2$ M^N state has been studied in great detail with a variety of techniques that include EPR, Mössbauer, ENDOR, and EXAFS spectroscopies.[1] The $S = {}^3/_2$ state of the isolated FeMoco has also been extensively studied. When redox-active dyes with midpoint potentials of ca. 0 to −100 mV vs SHE are added to the MoFe protein, the $S = {}^3/_2$ EPR signal disappears and a state designated M^{OX} is obtained. This one-electron oxidation reaction is fully reversible, and Mössbauer[15] and MCD[16] data have established that M^{OX} has a diamagnetic ground state. This reversible one-electron oxidation has also been demonstrated by dye or electrochemical oxidation of isolated FeMoco.[17,18]

Although M^{OX} and the corresponding oxidation state of isolated FeMoco have been extensively studied, the M^N/M^{OX} transition is unlikely to occur in vivo under substrate-reducing conditions. Rather, during substrate reduction, the $S = {}^3/_2$ M^N state is further reduced to an EPR-silent ($S > 1$) state that has been designated M^R.[15b] For the MoFe protein, this state can be produced only upon the addition of the physiological electron donor, the reduced Fe protein, and MgATP. Thus, the M^R substrate-reducing state of the M-center has never been produced electrochemically or with any artificial electron donor. The isolated FeMoco in NMF can be reversibly reduced by one electron below the $S = {}^3/_2$ state electrochemically,[18,19] but this state has not been spectroscopically examined, and its relationship to M^N is therefore not known.

The present study involves detailed characterization of M^N and M^R by Mössbauer spectroscopy. Previous Mössbauer studies of the $A\nu 1$[15b] and $Cp1$[15a] M-centers have revealed at least six Fe sites that were grouped into two classes according to the signs of the ^{57}Fe magnetic hyperfine coupling constants, A_{iso}. Thus, according to the Mössbauer studies,[15a] there are three sites, A^1-A^3, with negative A_{iso}, and three essentially equivalent B-sites having $A_{iso} > 0$. To keep the number of unknown parameters at a manageable number, the data were analyzed by assuming that all magnetic hyperfine tensors are isotropic (A_{iso}). Although there were some hints in the Mössbauer spectra for the presence of a seventh Fe site,[15a] the absorption associated with this putative site was masked to a large extent by the absorption contributed by the eight P-cluster irons.

Two developments have suggested to us to study again the Mössbauer spectra of M^N. First, ENDOR studies of $A\nu 1$ by Hoffman and collaborators[20] have provided a very detailed description of five ^{57}Fe magnetic hyperfine tensors (sites A^1, A^2, A^3, B^1, and B^2), including a full characterization of their orientations relative to the frame of the zero-field splitting tensor. Second, because FeMoco can be extracted from the MoFe protein and reinserted, it is possible to generate so-called isotopic hybrids of the MoFe protein that contain either the P-clusters ($^{56}M^{57}P$) or the M-centers ($^{57}M^{56}P$) selectively enriched with the Mössbauer isotope ^{57}Fe. Such hybrids have been studied for $Kp1$ with Mössbauer spectroscopy[21] and for $A\nu 1$ with ENDOR.[32] The availability of $A\nu 1$ $^{57}M^{56}P$ hybrids suggested to us that one should be able to detect the spectroscopic signature of the seventh iron site with Mössbauer spectroscopy. Moreover, given the precise **A**-tensors provided by ENDOR, a refined analysis of the Mössbauer spectra should reveal why only five distinct Fe sites are observed by ENDOR. Below we report that the seventh Fe site has unusually small **A**-tensor components,

(12) Palmer, G.; Multani, J. S.; Cretney, W. C.; Zumft, W. G.; Mortenson, L. E. *Arch. Biochem. Biophys.* **1972**, *153*, 325−332.
(13) Rawlings, J.; Shah, V. K.; Chisnell, J. R.; Brill, W. J.; Zimmermann, R.; Münck, E. *J. Biol. Chem.* **1978**, *253*, 1001−1004.
(14) Shah, V. K.; Brill, W. J. *Proc. Natl. Acad. Sci. U.S.A.* **1981**, *78*, 3438−3440.
(15) (a) Huynh, B. H.; Münck, E.; Orme-Johnson, W. H. *Biochim. Biophys. Acta* **1979**, *527*, 192−203. (b) Huynh, B. H.; Henzl, M. T.; Christner, J. A.; Zimmermann, R.; Orme-Johnson, W. H.; Münck, E. *Biochim. Biophys. Acta* **1980**, *623*, 124−138. (c) Rawlings, J.; Shah, V. K.; Chisnell, J. R.; Brill, W. J.; Zimmermann, R.; Münck, E.; Orme-Johnson, W. H. *J. Biol. Chem.* **1978**, *253*, 1001−1004. (d) Huynh, B. H.; Münck, E.; Orme-Johnson, W. H. *Biochim. Biophys. Acta* **1979**, *527*, 192−203. (e) Zimmermann, R.; Münck, E.; Brill, W. J.; Shah, V. K.; Henzl, M. T.; Rawlings, J.; Orme-Johnson, W. H. *Biochim. Biophys. Acta* **1978**, *537*, 185−207.
(16) Johnson, M. K.; Thomson, A. J.; Robinson, A. E.; Smith, B. E. *Biochim. Biophys. Acta* **1981**, *671*, 61−70.
(17) Burgess, B. K.; Stiefel, E. I.; Newton, W. E. *J. Biol. Chem.* **1980**, *255*, 353.
(18) Schultz, F. A.; Gheller, S. F.; Burgess, B. K.; Lowe, D. J.; Newton, W. E. *J. Am. Chem. Soc.* **1985**, *107*, 5364.
(19) Newton, W. E.; Gheller, S. F.; Feldman, B. J.; Dunham, W. R.; Schultz, F. A. *J. Biol. Chem.* **1989**, *264*, 1924−1927.
(20) True, A. E.; Nelson, M. J.; Venters, R. A.; Orme-Johnson, W. H.; Hoffman, B. M. *J. Am. Chem. Soc.* **1998**, *110*, 1935−1943.
(21) McLean, P. A.; Papaefthymiou, V.; Orme-Johnson, W. H.; Münck, E. *J. Biol. Chem.* **1987**, *262*, 12900−12903.
(22) Yoo, S. J.; Angove, H. C.; Burgess, B. K.; Hendrich, M. P.; Münck, E. *J. Am. Chem. Soc.* **1999**, *121*, 2534−2545.
(23) Yoo, S. J.; Meyer, J.; Münck, E. *J. Am. Chem. Soc.* **1999**, *121*, 10450−10451.
(24) Christiansen, J.; Goodwin, P. J.; Lanzilotta, W. N.; Seefeldt, L. C.; Dean, D. R. *Biochemistry* **1998**, *37*, 12611−12623.
(25) Brink, D. M.; Satchler, G. R. *Angular Momentum*; Clarendon Press: London, 1968.
(26) Arfken, G. *Mathematical Methods for Physicists*; Academic Press: New York, 1970.
(27) Münck, E. *The Porphyrins*; Academic Press: New York, 1979; Vol. IV, Chapter 8.
(28) In cases with superb resolution, such as that observed for the spectra of *E. coli* sulfite reductase, we found that the absorption of the siroheme iron and the [4Fe-4S] cluster were exactly in a 1:4 ratio. The spectra of reduced [3Fe-4S] clusters provide additional support for this assumption.
(29) A_{iso} of site A^4 is roughly −4 MHz. For sites with small and anisotropic A values the field dependence of the magnetic splitting can be quite complex. For instance, for weak applied magnetic fields the expectation value of the spin for the $M = -{}^1/_2$ state are $\langle S_i \rangle = g_i/4$, or $\langle S_x \rangle = -0.92$, $\langle S_y \rangle = -1.08$, and $\langle S_z \rangle = -0.50$. For $A_x/g_N\beta_N = -5.0$ T, for example, the internal magnetic field along x is about −4.5 T. As the applied field is increased, mixing of the $M = -{}^1/_2$ state with the $M = -{}^3/_2$ state increases $\langle S_x \rangle$ to ca. −1.4 at 8.0 T (see also Figure 8), i.e., B_{int} increases to about −7.0 T. However, since B_{int} is negative, it is opposed by the applied field. Consequently, $|B_{eff}|$, the quantity determining the magnetic splitting, increases at low field and decreases at high field. This pattern of increasing and decreasing splittings is orientation- and field-dependent, and since the A values are small, outward and inward moving features are not resolved at all. However, the splitting pattern is still easily distinguished from that resulting from a site with positive A values; for the latter, the magnetic splittings will always increase with increasing applied field.
(30) Footnote 21 of ref 20.
(31) Kent, T. A.; Huynh, B. H.; Münck, E. *Proc. Natl. Acad. Sci. U.S.A.* **1980**, *77*, 6574−6576.
(32) Lee, H.-I.; Hales, B. J.; Hoffman, B. M. *J. Am. Chem. Soc.* **1997**, *119*, 11395−11400.

and moreover, we present evidence that the ENDOR resonances attributed to site B^1 represent two identical Fe sites.

We have also studied in more detail the turnover state, M^R. Our data show that the increase in isomer shift between M^N and M^R is substantially smaller than that observed between M^{OX} and M^N. Furthermore, the high-field Mössbauer spectra of M^R were found to be quite similar to those observed for M^N, suggesting that the spin structure of the Fe segment of the M-center is similar in both states. These observations can be rationalized by assuming that the extra electron of M^R resides essentially on the molybdenum.

In the absence of Fe protein and MgATP, reduction of the M-centers beyond the state M^N has not yet been accomplished. We have recently produced the all-ferrous state of the [4Fe-4S]-containing Fe protein[22] and the diferrous state of a [2Fe-2S] ferredoxin from *Aquifex aeolicus*[23] by radiolytic reduction at 77 K in a synchrotron X-ray beam. The reduced states observed for these two proteins were found to be indistinguishable from those attained by chemical reduction at room temperature. We were curious to know whether radiolytic reduction of the MoFe protein would further reduce the M-center, and if so, whether the turnover state M^R or some other reduced cluster would be observed. We report here the observation of a new state, M^I, with integer electronic spin $S > 1$ that is at the same oxidation level as M^R, i.e., one electron further reduced than M^N. The isomer shift of M^I was found to be larger than that of M^R, suggesting that the reduction occurs in the Fe portion of the cluster.

Materials and Methods

The ΔnifB strain DJ1143 that was used to purify the FeMoco-deficient His-tagged MoFe protein was kindly provided by Prof. Dennis Dean, Virginia Tech, and purified as described by Christiansen et al.[24] ^{56}Fe FeMoco-deficient His-tagged MoFe protein (0.75−0.8 mg/mL) in 25 mM Tris-HCl, pH 7.4 buffer, 1 mM dithionite, and NaCl < 50 mM was reconstituted by the addition of excess isolated ^{57}Fe FeMoco. The final NMF concentration was <4 μL/mL. Excess FeMoco was washed from the protein bound to a Q Sepharose column.[24] The reconstituted $^{57}M^{56}P$ MoFe protein had a final activity of 1400 nmol of H_2 min^{-1} mg^{-1} (70% of the value reported for the WT His-tagged protein[24]). Because only the ^{57}M-centers are being monitored in this study, the presence of some ^{56}FeMoco-deficient MoFe protein does not interfere.

Mössbauer and EPR samples were prepared in glass centrifuge and EPR tubes fitted with septa and attached to a Vac/Gas manifold under N_2. Samples were mixed manually and transferred using anaerobic Hamilton syringes fitted with long needles. Mössbauer and EPR parallel samples were frozen simultaneously. The $^{57}M^{56}P$ MoFe protein concentration was 0.22 mM. Turnover samples contained 0.214 mM Fe protein, 30 mM sodium dithionite, 2.5 mM ATP, 3.5 mM Mg^{2+}, 31 mM creatine phosphate, 27 units/mL creatine phosphokinase, 50 mM Tris-HCl, pH 7.4, and 280 mM NaCl. Turnover samples were frozen 2 min after the final addition of the Fe protein. The percent reduction was determined by monitoring the disappearance of the $S = {}^3/_2$ EPR signal.

Irradiation Samples. EPR and Mössbauer samples for irradiation in a synchrotron X-ray beam were prepared in a Vacuum Atmospheres drybox under Ar. Sodium dithionite was removed from the protein samples using a Sephadex G-25 column equilibrated with 50 mM Tris-HCl, pH 8.0, and 300 mM in NaCl. Glycerol was added to give a final concentration of 10% (v/v). Final concentrations of ^{56}Fe MoFe protein, ^{57}Fe MoFe protein, and ^{57}Fe FeMoco-deficient His-Tagged MoFe protein were 29, 29.2, and 32.2 mg/mL, respectively. Blank samples of glycerol were also used as a control. Following irradiation, the dithionite-free MoFe protein Mössbauer sample was shipped to Irvine, thawed, and assayed to give ca. 82% of its original activity.

Spectroscopy. Mössbauer spectra were recorded with two spectrometers operating in the constant acceleration mode. High-field spectra (0.15−8.0 T) were recorded using a Janis Research Super-Varitemp Dewar equipped with a superconducting magnet. Isomer shifts are quoted relative to Fe metal at 298 K. Mössbauer spectral simulations were generated using the WMOSS software package (WEB Research, Edina, MN).

Results

Methods of Analysis. The Mössbauer spectra of the $S = {}^3/_2$ state of the M-center can be described with the spin Hamiltonian:

$$H = \mathbf{S}\cdot\mathbf{D}\cdot\mathbf{S} + \beta\mathbf{S}\cdot\mathbf{g}\cdot\mathbf{B} + \sum_{i=1}^{7}\{\mathbf{S}\cdot\mathbf{A}(i)\cdot\mathbf{I}(i) + H_Q(i) - g_N\beta_N\mathbf{B}\cdot\mathbf{I}(i)\} \quad (1)$$

In eq 1, **D** is the traceless zero-field splitting tensor described by the parameters D and E/D. EPR, Mössbauer, and ENDOR studies of dithionite-reduced $A\upsilon 1$ have established that $D = 6$ cm^{-1} and $E/D = 0.05$.[5,15,20] Moreover, EPR studies have shown that the electronic **g**-tensor is almost isotropic,[5] with $g_x = g_y = 2.00$ and $g_z = 2.03$. The quoted value for E/D gives rise to the prominent EPR signal of the $M = \pm {}^1/_2$ ground Kramers doublet with effective $g = 4.32$, 3.68, and 2.01. The $\mathbf{A}(i)$ are the magnetic hyperfine tensors; their principal axis frames are rotated by Euler angles (α_A, β_A, γ_A) relative to the frame defined by the zero-field splitting tensor. The rotations used here are those of Brink and Satchler[25] and Arfken;[26] for instance, if $A_{x'x'}$, $A_{y'y'}$, and $A_{z'z'}$ are the principal axis values of **A**, the transformation $\mathbf{R}^{-1}\mathbf{A}\mathbf{R}$ expresses the **A**-tensor in the principal axis frame of the **D**-tensor, with the rotation matrix **R** given by eq 4.80 of Arfken. $H_Q(i)$ describes the interaction of the nuclear quadrupole moment with the electric field gradient (efg) tensor. In its principal axis form, H_Q, for each site i, is written as

$$H_Q = (eQV_{\zeta\zeta}/12)[3\mathbf{I}_\zeta^2 - 15/4 + \eta(\mathbf{I}_\xi^2 - \mathbf{I}_\eta^2)] \quad (2)$$

Without loss of generality, the asymmetry parameter $\eta = (V_{\xi\xi} - V_{\eta\eta})/V_{\zeta\zeta}$ of the efg tensor can be constrained to $0 < \eta < 1$. The set of Euler angles (α_{efg}, β_{efg}, γ_{efg}) rotates the principal axis frame of the efg tensor, (ξ,η,ζ), into the frame of the zero-field splitting tensor.

The magnetic splittings of the Mössbauer spectra are controlled by the internal magnetic fields $\mathbf{B}_{int}(i) = \langle S\rangle\cdot\mathbf{A}(i)/g_n\beta_n$, where $\langle S\rangle$ is the expectation value of the cluster spin. At low temperature, e.g. at 4.2 K, the electronic spin relaxes slowly compared to the nuclear precession times, and $\langle S\rangle$ is the expectation value of S taken for the $M = \pm {}^1/_2$ ground doublet; at 4.2 K there are very minor (<2%) contributions from the $M = \pm {}^3/_2$ doublet. At 150 K, in contrast, the electronic system relaxes fast, and $\langle S\rangle$ corresponds to the thermally averaged spin, $\langle S\rangle_{th}$ (see ref 27). Because D, E/D, and five **A**-tensors are known, the internal fields for all directions of the applied field **B** are essentially determined. The magnetic splittings of the Mössbauer spectrum are determined by the effective field $\mathbf{B}_{eff} = \mathbf{B}_{int} + \mathbf{B}$. By comparing the magnitude of $\mathbf{B}_{eff}$ for different applied fields, the sign of $\mathbf{B}_{int}(i)$ and therefore the sign of $\mathbf{A}(i)$ can be determined. For the spectral simulations we have assumed that the recoil-less fractions of all iron sites are the same at 4.2 K. This seems to be a very good assumption, and during the past 25 years we have not found in our laboratory a single instance where this assumption was not valid at low temperature.[28] The assumption of equal recoil-less fractions implies that each iron site contributes the same spectral area.

Results for M^N. We have studied the Mössbauer spectra of MoFe protein, in the state M^NP^N, with the M-centers selectively

Table 1. 4.2 K Hyperfine Parameters of the $S = {}^3/_2$ State of M^N [a]

	A^1	A^2	A^3	A^4	B^1	B^2
δ (mm/s)	0.39	0.48	0.39	0.41	0.33	0.50
ΔE_Q (mm/s)	−0.69	−0.94	−0.56	0.68	−0.66	−0.65
η	1	1	1	1	0.9	1
α_{efg} (deg)	120	115	60	0	40	6
β_{efg} (deg)	0	20	30	130	125	70
γ_{efg} (deg)	0	4	176	30	0	0
$A_{x'}$ (MHz)	−13.8 (−13)	−17.3 (−18)	−13.9 (−14)	−1.5	+11.7 (11)	+8.5 (11)
$A_{y'}$ (MHz)	−21.1 (−21)	−15.1 (−14)	−11.6 (−12)	−9.5	+14.1 (14)	+11.0 (9)
$A_{z'}$ (MHz)	−19 (−10)	−19 (−19)	−10 (−10)	0	+9.2 (9)	+8.2 (19)
A_{iso} (MHz)	−18.0	−17.1	−11.8	−3.7	+11.7	+9.3
α_A (deg)	20 (15)	13 (10)	25 (30)	112	0 (0)	9 (12)
β_A (deg)	0 (0)	22 (15)	0 (0)	60	56 (45)	0 (0)

[a] Shown in italics in parentheses are the ENDOR values of True et al.[20] For the simulations of the spectra shown in Figures 1−5 the zero-field splitting parameters $D = 6.0$ cm^{-1} and $E/D = 0.055$ were used. $\Delta E_Q = eQV_{\zeta\zeta}/12(1 + {}^1/_3\eta^2)^{1/2}$; $A_{iso} = (A_{x'} + A_{y'} + A_{z'})/3$; $(x',y'z')$ is the principal axis system of the **A**-tensor. (α_A,β_A) describes the orientation of this system relative to that of the **D**-tensor.

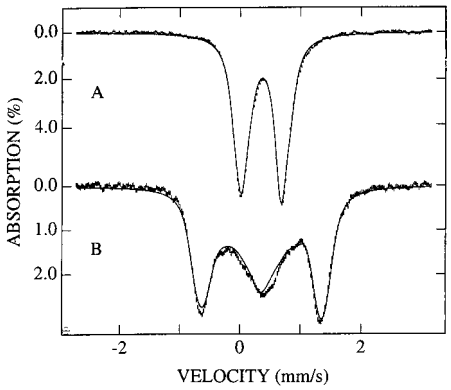

Figure 1. Mössbauer spectra of the M-center recorded at 150 K in zero field (A) and in the presence of an 8.0-T field (B) applied parallel to the observed γ-rays. The solid lines are spectral simulations based on eq 1 and using the parameters of Table 1.

enriched with ^{57}Fe. In our samples, the P-clusters contain ^{57}Fe in natural abundance (2.2%), and if we assume a ^{57}Fe enrichment of ca. 90% for the M-centers, then approximately 2.7% of the total Mössbauer absorption belongs to P^N. P^N is diamagnetic, and its spectral signature is well known from previous studies,[15a] allowing us to remove its contribution from the data using simulated spectra.

Figure 1A shows a zero-field Mössbauer spectrum recorded at 150 K. This spectrum consists of one doublet with average $\Delta E_Q = 0.68$ mm/s and $\delta = 0.36$ mm/s, with a line width of 0.28 mm/s. To assess whether one can recognize any subsites, in particular the tetrahedral iron bound to αCys275, we have removed the line width contribution of the ^{57}Co(Rh) source by a Fourier transform technique. This technique, successfully applied previously to resolve subsites of the P-cluster,[15a] reduces in the present case the line width by nearly a factor 2. Nevertheless, we were unable to recognize subsites in the transformed spectrum. Although the spectrum of Figure 1A displays an apparently well-defined doublet, it can accommodate sites with ΔE_Q values ranging from 0.55 to 0.93 mm/s. As stated previously,[15a] the quadrupole splittings are nearly independent of temperature; thus, ΔE_Q decreases by less than 0.05 mm/s between 80 and 180 K.

Figure 1B shows a 150 K spectrum recorded in an 8.0-T field applied parallel to the observed γ-radiation. The spectrum shown was obtained under conditions where the electronic spin relaxes fast compared to the nuclear precession frequencies. The symmetric features of the spectrum imply that the asymmetry parameter η of the efg tensors of nearly all sites are near the rhombic limit, $\eta = 1$. The solid lines drawn through the spectra

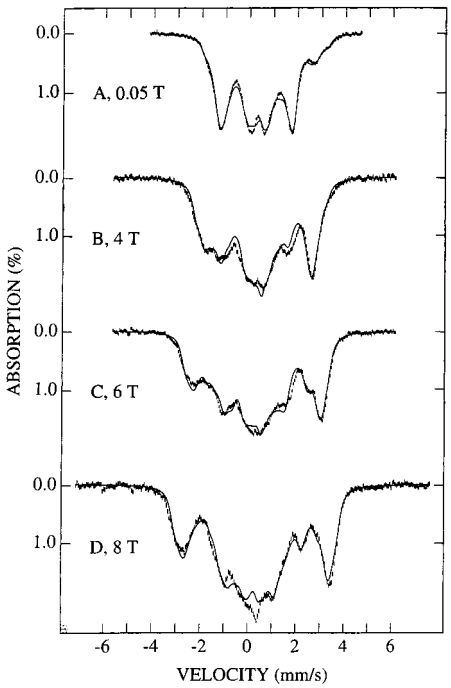

Figure 2. 4.2 K Mössbauer spectra of the $S = {}^3/_2$ state of M-center recorded in parallel applied magnetic fields as indicated. The solid lines are spectral simulations for seven sites using the parameters listed in Table 1.

of Figure 1 are spectral simulations based in eq 1 using the parameters listed in Table 1.

Figure 2 shows 4.2 K Mössbauer spectra recorded in applied magnetic fields as indicated. The solid lines drawn through the spectra are simulations based on eq 1, using the parameters of Table 1. Since these spectra depend on as many as 84 hyperfine parameters, we describe in the following how the spectral decomposition was accomplished. To analyze the spectra of Figure 2, we used the five **A**-tensors of True et al.[20] From the analysis of the spectra of Figure 1, we were able to narrow the range of ΔE_Q values, and moreover, the spectrum of Figure 1B fixes the η values near their rhombic limit. With these constraints we were left to find the spectral features of the seventh site, and to determine the orientations of seven efg tensors.

Figure 3 shows the spectra of Figure 2A and D together with spectral simulations of the previously identified six Fe sites. Clearly, the central region of the spectra contains absorption features, ca. 15% of total Fe, not accounted for by the theoretical curves. These features correspond to one iron site (ca. 14−15%

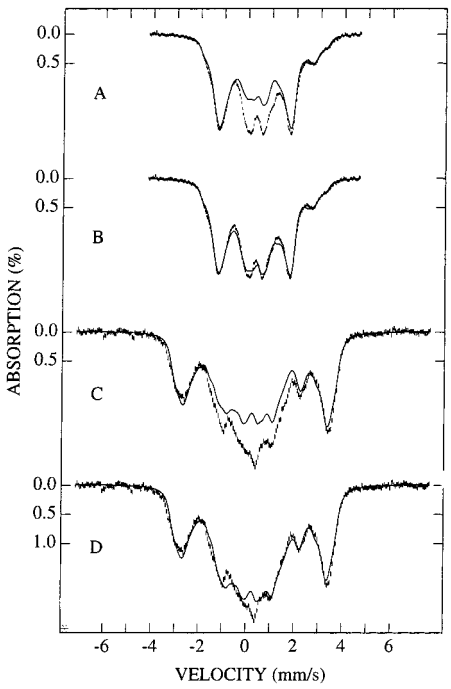

Figure 3. Comparison of simulations of the 4.2 K spectra of M^N using seven sites (B,D) with simulations for six sites (A,C) using the parameters for A^1-A^3, B^1, and B^2 (B^1 representing two sites).

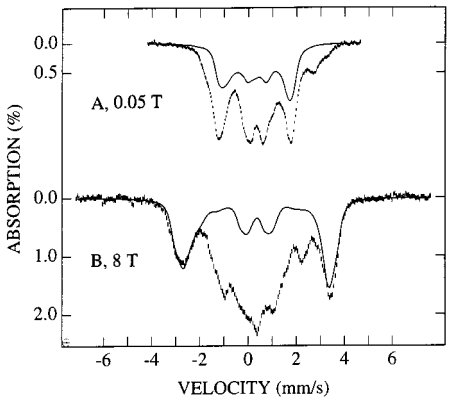

Figure 4. Simulations for sites B^1 (two irons) and B^2 illustrated for the 0.05- and 8.0-T spectra (same data as Figure 2A,D). Theoretical curves represent three-sevenths of the total absorption.

of the total absorption) with magnetic hyperfine interactions substantially smaller than those observed for the other six sites.

Figure 4A and B shows the spectra of Figure 2A and D together with the theoretical curves of the *B*-sites. These spectra, together with the set of spectra shown in Figure 2, demonstrate that the outermost features of the 8.0-T spectrum are entirely due to sites with positive $\mathbf{B}_{int}$, i.e., *B*-sites. Our simulations of the 8.0-T spectrum readily establish that three Fe sites contribute. Since only two ENDOR resonances with positive *A* values were observed in the well-resolved spectra of $A\nu1$,[20] one set of ENDOR resonances must represent two equivalent sites. The best fits to the Mössbauer spectra were obtained by assigning two sites to B^1; assignment of two sites to B^2 produced fits of decidedly lower quality. True et al.[20] have tentatively assigned $|A_{z'}| = 10$ MHz to site A^1 and $|A_{z'}| = 19$ MHz to B^2, but they indicated that the reverse assignment is also possible. Although we have obtained slightly better fits with the reverse assignment, the improvement is within the uncertainties of multiparameter fits; this is not unexpected because the anisotropy of the

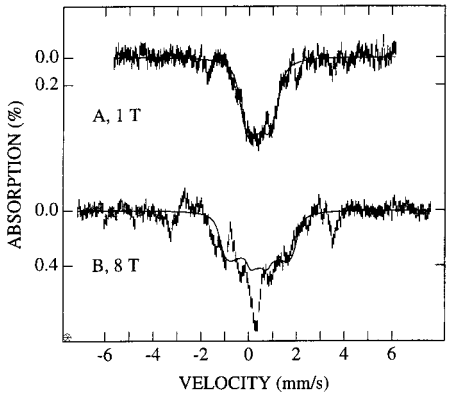

Figure 5. Difference spectra, meant to indicate the contribution of site A^4, obtained by subtracting the spectral simulations of sites A^1-A^3, B^1, and B^2 from the raw data. The features around +3.5 and −3.2 mm/s in spectrum B are artifacts of the subtractions. The solid lines are spectral simulations for site A^4 using the parameters of Table 1. See also Note Added in Proof.

electronic system statistically favors the *xy*-plane, and thus the Mössbauer spectra are much less sensitive to $A_{z'}$ than to $A_{x'}$ and $A_{y'}$.

As indicated above, the absorption of the seventh Fe site is confined to the central regions of the spectra. To assess its parameters we have subtracted from the raw data the simulated spectra of A^1, A^2, A^3, B^1, and B^2; the 1.0- and 8.0-T spectra of the seventh site are shown in Figure 5. While this procedure yields spectra indicating the velocity range to which the absorption of the seventh site is confined, small errors resulting from imperfect simulations of the spectra of the other six sites introduce uncertainties that impose severe limits on the determination of the **A**-tensor of the seventh site. However, the data set shows that the **A**-tensor components, or more precisely, the largest component of **A**, is negative and has magnitude 7−10 MHz. $A_{x'}$ and $A_{z'}$ are smaller in magnitude and probably also negative.[29] Because $A_{y'}$ dominates, $A_{iso} = (A_{x'} + A_{y'} + A_{z'})/3$ is negative, and therefore the seventh site is an *A*-type site which we label as A^4.

Although simulation of the M-center spectra requires specification of 84 hyperfine parameters, the fits are reasonably unambiguous because some spectral features are quite well resolved and because five **A**-tensor sets are known from ENDOR. Our final parameter set was obtained by individually simulating the spectra of Figures 1 and 2, recognizing the crucial features of each spectral component, and then group-fitting the whole data set using a least-squares fitting routine. For these group fits we have initially used the published **A**-tensors, allowing variations of the other parameters within bounds that seemed appropriate from the knowledge gained by simulating individual spectra. In a later stage we were able to improve the fits by allowing variations of the **A**-tensor components and rotation angles that were compatible with the stated uncertainties of the ENDOR study of True et al.[20] For site B^2 we found it advantageous to interchange the $A_{x'}$ and $A_{y'}$ values (8.9 and 11 MHz) of True *et al.*; while this produced better fits, the improvement is not so pronounced as to challenge the ENDOR results. It is very difficult to estimate the uncertainties, in particular those associated with the rotations of the efg tensors. The quadrupole splittings are confined, from the spectrum of Figure 1A, to $0.55 < |\Delta E_Q| < 0.93$ mm/s, and the spectrum of Figure 1B shows that essentially all η values are close to $\eta = 1$. Because the **A**-tensors of sites A^1-A^3, B^1, and B^2 are known from ENDOR with good precision, the quoted orientations of

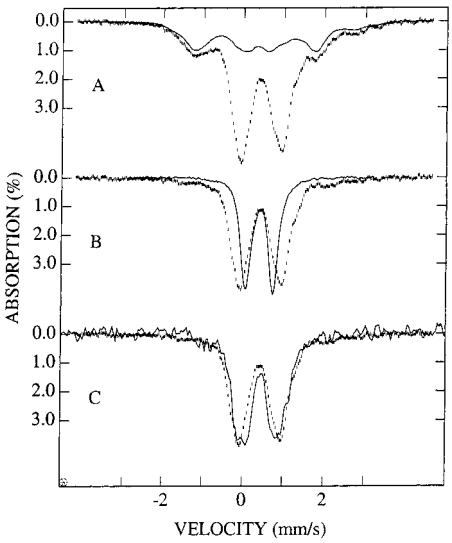

Figure 6. Mössbauer spectra of the turnover complex (A,B) and radiolytically reduced M-center (C). (A) 4.2 K spectrum, recorded in a 0.05-T parallel field, of turnover complex of a $^{57}M^{56}P$ sample. 60% of the absorption of the sample is contributed by M^R and 40% belongs to M^N; the latter contribution is outlined by the solid line (same *experimental* spectrum as shown in Figure 2A). (B) Spectrum of M^R (hash marks) obtained from spectrum A by subtracting the contribution of M^N. The solid line is a spectrum of M^N taken at 150 K. (C) 0.05-T spectrum of M^I obtained by subtracting the contribution of M^N (61%) from the spectrum of the irradiated sample (solid line); hash marks represent a spectrum of M^R (same as B). These preliminary data were recorded at 4.2 K for a $^{57}M^{56}P$ sample.

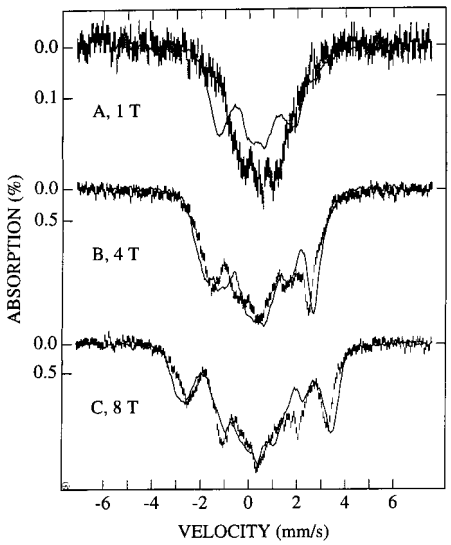

Figure 7. 4.2 K spectra (hash marks) of M^R recorded in parallel applied fields of 1.0 T (A), 4.0 T (B), and 8.0 T (C). Spectra shown were obtained by subtracting the contributions (40%) of M^N. For comparison, the corresponding spectra of M^N (solid lines) are shown.

the efg tensors of these sites should be roughly correct. The orientation of the efg tensor of A^4 is very uncertain.

Results for M^R. In the course of the present study, we have studied one sample of $^{57}M^{56}P$ MoFe protein prepared under turnover conditions (see Materials and Methods). Figures 6 and 7 show Mössbauer spectra of this sample. The spectrum of Figure 6A, recorded at 4.2 K in a parallel field of 0.05 T, exhibits contributions from two distinct species. One species, accounting for ca. 40% of the ^{57}Fe, belongs to the $S = {}^3/_2$ form of M^N; its contribution is indicated by the solid line. A second species contributes quadrupole doublets; this species represents the turnover complex M^R described previously for $^{57}M^{57}P$ samples of *Av*1[5] and *Cp*1.[15b] The spectrum of Figure 6B (hash marks) was obtained by subtracting from spectrum A the contribution of M^N. For comparison of the doublet features of M^R and M^N, Figure 6B shows also a spectrum of M^N (solid line); because M^N exhibits paramagnetic hyperfine structure at 4.2 K, we have used the 150 K spectrum of M^N, shifting it by 0.05 mm/s to higher energy to account for the second-order Doppler shift between 4.2 and 150 K. Comparison of the spectra of M^N and M^R shows that the quadrupole splittings of nearly all Fe sites have changed upon formation of the turnover complex. Although a unique decomposition of the M^R spectrum into individual doublets is not possible, the M^R spectrum can be synthesized by a superposition of doublets such that its features are well reproduced. From such syntheses we found that δ_{av} has to be between 0.43 and 0.44 mm/s. (The value $\delta =$ 0.36 mm/s listed Table 1 of ref 15b is a typographical error.) Compared to the isomer shift change between M^{OX} ($\delta_{av} = 0.35$ mm/s, ref 15b) and M^N ($\delta_{av} = 0.41$ mm/s), δ_{av} changes little between M^N and M^R. We address the point below.

Figure 7A−C shows 4.2 K spectra of M^R (hash marks) obtained in parallel applied fields of 1.0, 4.0, and 8.0 T. The spectra shown were obtained by subtracting from the raw data the corresponding spectrum of M^N, using the fraction (40%) obtained from the analysis of the 0.05-T spectrum shown in Figure 6A. The ground-spin multiplet of M^R has integer electronic spin $S > 0$. That M^R has integer spin follows from three observations. First, the 0.05-T spectrum of M^R exhibits quadrupole doublets rather than magnetically split components, i.e., $\langle S \rangle \approx 0$. Second, the splitting patterns observed in Figure 7 show that the electronic system becomes polarized with increasing applied field. It could be argued that a doublet pattern is observed at low field because of fast electronic relaxation (which we have never observed at 4.2 K for protein-bound Fe). However, spectra recorded at 4.0 T at 4.2 and 1.5 K (not shown) exhibited the same splittings, showing that the electronic spin relaxes slowly at 4.2 K. Third, no signal attributable to M^R was observed in parallel or transverse EPR at Q- and X-band.

Figure 7B,C shows that the high-field spectra of M^R (hash marks) and M^N (solid lines) are strikingly similar. This similarity suggests that the spin-coupling within the 7-Fe segment of the cofactor is essentially the same in M^N and M^R. This similarity, and isomer shift considerations, suggest to us that one should consider the possibility that the additional electron is accommodated at the molybdenum site; we will discuss this point below.

A Reduced State of M Produced by Radiolytic Reduction at 77 K. We have recently produced novel oxidation states of [2Fe-2S] and [4Fe-4S] clusters by radiolytic reduction of samples at 77 K in a synchrotron X-ray beam.[22,23] Because all attempts to reduce the M-center, in the absence of Fe protein and MgATP beyond M^N have failed in the past, we have attempted to achieve reduction by exposing the MoFe protein at 77 K to synchrotron X-rays. In two experiments we observed a decline of the $S = {}^3/_2$ EPR signal by ca. 50% after irradiation of the MoFe protein in the state M^NP^N at 77 K, suggesting that the M-center had been reduced; no new species exhibiting EPR signals other than those attributable to radicals were observed. Activity assays (see Materials and Methods) demonstrated that these changes were reversible. Encouraged by these results, we have irradiated a $^{57}M^{56}P$ sample in the state M^NP^N. Here we report a preliminary result. Inspection of a 4.2 K Mössbauer spectrum, recorded in a parallel field of 0.05 T, showed that spectral component M^N had declined to 61% as the result of

the irradiation. Removal of the remaining absorption due to M^N yielded the spectrum of Figure 6C. The irradiation product, labeled M^I, has δ between 0.45 and 0.46 mm/s and thus represents a state more reduced than M^N. Preliminary studies in strong applied fields show that M^I must have integer electronic spin $S > 0$. The 6.0-T spectrum of M^I (not shown) exhibits paramagnetic hyperfine structure with a splitting pattern that differs from that observed for M^R, suggesting that M^R and M^I have different spin structures.

Discussion

Cluster-State M^N. We have provided here a set of hyperfine parameters for M-cluster-state M^N that fits the low- and high-temperature Mössbauer spectra very well. In particular, we have been able to identify site A^4 of the M-center that had previously not been detected by either ENDOR or Mössbauer spectroscopy. Although we had indicated that we suspected a seventh iron site with unusual magnetic hyperfine interactions,[30] the presence of the P-cluster absorption masked its spectral features to a large extent, and thus we were not in the position to argue persuasively for the presence of such a site. In our Mössbauer study of isolated FeMoco, published in 1978, we suggested that a feature (indicated by the brackets in Figure 2A and B of ref 15c) might represent a doublet belonging to M^{OX} of a partially oxidized sample. We understand now that this feature results from the innermost lines of the magnetic components A^1-A^3, B^1, and B^2, elevated by an underlying broad feature belonging to A^4. Thus, in our present understanding, the cofactor spectra of ref 15c represent pure samples of FeMoco in the $S = {}^3/_2$ form.

In 1978, we did not suspect the presence of an iron site with very small hyperfine interactions. However, our subsequent studies of oxidized [3Fe-4S] clusters alerted us to the possibility that sites of polynuclear clusters may exhibit vanishingly small magnetic hyperfine interactions even though their intrinsic A values may not be unusual. Thus, in a spin-coupled cluster, the magnetic hyperfine interaction of a local site is proportional to the projection of the local spin onto the direction of the cluster spin. The spin of a local site may be oriented nearly perpendicular to the cluster spin, as observed for $[3Fe\text{-}4S]^+$ clusters.[31] The small hyperfine interactions of the A^4-site undoubtedly reflect such a situation. Because of its small and anisotropic **A**-tensor, the A^4-site has eluded detection by ENDOR spectroscopy. As pointed out above, it is exceedingly difficult to prepare faithful representations of the spectra of site A^4 by subtracting the simulated contributions of the other six sites. Therefore, we have not been able to determine the **A**-tensor components of A^4 with precision; however, we are certain that A_{iso} is negative (roughly -4 MHz), and moreover, we have convinced ourselves that the **A**-tensor is quite anisotropic.

The theoretical curves shown in Figures 1 and 2, all computed with the parameter set of Table 1, match the data quite well. In our experience, these fits are about as good as one can hope to obtain, given that the spectra depend on as many as 84 hyperfine parameters. We have not yet been able to assign any of the sites identified by ENDOR and Mössbauer spectroscopy to a particular crystallographic site; even the unique tetrahedral iron coordinated by αCys 275 does not provide a spectral signature that distinguishes it clearly from the trigonal iron sites. To link the spectroscopic information with the crystallographic sites, two directions of future research could prove fruitful. First, one may be able to perturb a particular site by site-directed mutagenesis without affecting the properties of the other sites in a major way. Second, bioinorganic chemists may learn how to assemble FeMoco by fusion of the subcubes selectively enriched with ^{57}Fe; such an accomplishment, still a daunting task, would enable one to assign the spectroscopically identified sites and the subcubes (if the Fe atoms do not exchange).

The X-ray structures of the MoFe protein[8-11] show that the M-center is a unique metal cluster of composition [Mo-7Fe-9S-homocitrate] containing six distorted trigonal iron sites plus one iron tetrahedrally coordinated to three sulfides and one sulfur from αCys275. That the six "trigonal" iron sites are distorted is immediately obvious from an inspection of Table 1. Thus, all iron sites have efg tensors exhibiting rhombic symmetry, i.e., $\eta = 1$. Interpretation of the hyperfine parameters obtained for M^N from Mössbauer and ENDOR spectroscopy is difficult for a variety of reasons. The isomer shifts are very unusual, reflecting either an environment not yet captured by any synthetic model or extensive delocalization among pairs (or larger assemblies) of metals. The system is exchange coupled, and since at least seven spins participate in the coupling (assuming a diamagnetic Mo^{4+} as suggested from the interpretation of the ENDOR data[32]), the magnetic hyperfine couplings are modified relative to their intrinsic values by unknown exchange interactions between sites in unknown oxidation states. Presently, we cannot offer a conclusive interpretation of the hyperfine parameters in terms of iron oxidation states and an exchange-coupling model. However, a variety of interesting features have emerged from our studies, and in the following we discuss briefly what these features might tell us about the cluster. As more information about the cofactor emerges, researchers may be able to integrate our results into a more comprehensive assessment of the electronic structure of the M-center.

Since the first description of the Mössbauer spectra of the M-center, the isomer shifts have been difficult to interpret in structural and electronic terms. Isomer shifts depend on the coordination environment and the oxidation state. For a fixed coordination, δ is a reliable oxidation state marker, as has been amply demonstrated for clusters with a [4Fe-4S] core[22,33] and many other compounds. Unfortunately, little information is available for iron compounds with trigonal sulfur coordination. ENDOR studies[32] of the $S = {}^1/_2$ state of CO-inhibited M-centers (this state is thought to be isoelectronic with M^N; see ref 32) and M^N have led to the suggestions that the molybdenum site of the $S = {}^3/_2$ state of the cofactor is Mo^{4+} and that the Mo-7Fe-9S core contains six Fe^{2+} and one Fe^{3+}. The conclusion regarding the iron oxidation states was based on a rough estimate of spin projection factors without the benefit of a detailed spin-coupling model and without knowledge of intrinsic A values of trigonally coordinated sulfur complexes.

Power and co-workers[34] have synthesized a high-spin Fe^{2+} complex, $[Fe(SC_6H_2\text{-}2,4,6\text{-}t\text{-}Bu_3)_3]^-$ (**1**), for which a trigonal thiolate coordination is enforced by use of sterically encumbered ligands. This complex has $\Delta E_Q = 0.81$ mm/s, which fits well to the average $\Delta E_Q = 0.69$ mm/s of the cofactor sites (most high-spin ferrous complexes have ΔE_Q values between 2.5 and 3.3 mm/s). The complex exibits $\delta = 0.57$ mm/s at 4.2 K, which is about 0.13 mm/s smaller than the shift of tetrahedral $Fe^{2+}S_4$ compounds but still noticeably above $\delta_{av} = 0.41$ mm/s of M^N. The reader may wonder whether the thiolate coordination imparts an isomer shift significantly different from that of the

(33) Holm, R. H. In *Advances in Inorganic Chemistry*; Cammack, R., Ed.; Academic Press: New York, 1992; Vol. 38, pp 1−62.

(34) MacDonnell, F. M.; Rohlandt-Senge, K.; Ellison, J. J.; Holm, R. H.; Power, P. P. *Inorg. Chem.* **1995**, *34*, 1815−1822.

(35) Schultz, C.; Debrunner, P. G. *J. Phys. C6* **1976**, *37*, 153−158.

(36) The isomer shift of Fe^{3+} rubredoxin from *Clostridium pasteurianum* has been reported to be 0.32 mm/s.[35] We have recently studied the same protein and obtained $\delta = 0.24 \pm 0.01$ mm/s.[37]

μ_3- sulfido coordination observed for the M-center. We expect such differences to be minor. For instance, the tetrahedral Fe^{3+}-$(Cys)_4$ sites of rubredoxin ($\delta = 0.24$ mm/s[35−37]), desulforedoxin ($\delta = 0.25$ mm/s[38]), and $Fe^{3+}(RS)_4$ model complexes ($\delta = 0.25$ mm/s[39]) exhibit δ values similar to those of the $Fe^{3+}(S_2)(Cys)_2$ sites of $[2Fe\text{-}2S]^{2+}$ clusters ($\delta = 0.25-0.27$ mm/s[40]).[41] While the δ values of trigonally coordinated Fe^{2+} complexes can be expected to vary somewhat with the coordination symmetry, we expect isomer shifts that cluster closely around the δ value of the Power complex. Unfortunately, the Fe^{3+} analogue of the Power complex has not been prepared. Taking into account that the isomer shift generally decreases with decreasing coordination number and observing that the isomer shift of **1** is ca. 0.13 mm/s smaller than those of tetrahedral $Fe^{2+}S_4$ complexes, we estimate that the δ values of a ferric analogue of the Power complex would be about 0.10−0.15 mm/s. From this perspective, the isomer shift of M^N, $\delta_{av} = 0.41$ mm/s, is roughly $Fe^{2.4+}$. (A δ value of 0.41 mm/s for a tetrahedral site such as the Fe coordinated to αCys 275 would correspond to $Fe^{2.5+}$.) Thus, the seven Fe sites of M^N appear to be roughly three oxidation equivalents above all-ferrous, suggesting, as an alternative to the proposal by Lee et al.,[32] that the cofactor core of M^N might be formulated as (Mo^{4+}-$4Fe^{2+}$-$3Fe^{3+}$). This description may also aid us with the interpretation of the magnetic hyperfine tensors of M^N. (Three intercubane Fe−Fe distances of M^N are rather short, ≈2.61 Å,[11] raising the question of whether incipient metal−metal bonds lower the value of δ through screening effects. In the absence of suitable model systems this question is difficult to answer. We note, however, that the δ values of the all-ferrous [4Fe-4S] cluster of the nitrogenase Fe protein are essentially the same as those observed for monomeric $Fe^{2+}S_4$ complexes,[22] despite the presence of four Fe−Fe distances substantially shorter, ≈2.53 Å,[62] than those reported for M^N. Further, the Fe−Fe distances of two conformers of an isopropoxide-bridged Fe^{2+}−Fe^{3+} complex[47] differ by 0.124 Å (2.624 vs 2.749 Å); within the uncertainties the average δ values of both complexes are the same.)

For the interpretation of the magnetic hyperfine interactions of M^N, knowledge of both the spin coupling of the [Mo-7Fe-9S] cluster and the intrinsic magnetic hyperfine tensors is required. In the following we discuss briefly some pertinent points. In an exchange-coupled cluster the observed **A**-tensors, $\mathbf{A}(i)$, are related to the local **A**-tensors, $\mathbf{a}(i)$, by $\mathbf{A}(i) = K_i\mathbf{a}(i)$, where the K_i are spin projection factors (see Mouesca et al.[42]) that depend on the details of the exchange-coupling scheme. We are currently studying the aforementioned Power complex (**1**). Our preliminary findings[43] are that the axial **A**-tensor of this high-spin ferrous complex is highly anisotropic ($|A_z/A_x| \approx 4$). The isotropic part of the **A**-tensor, $A_{iso} \approx -15$ MHz, is found to be substantially smaller than the corresponding $A_{iso} \approx -22$ MHz of tetrahedral $Fe^{2+}S_4$ sites. While the spin projection factors K_i modify the magnitudes of the A values, they do not change the anisotropy (as long as only isotropic exchange matters and mixing of multiplets by zero-field splitting terms is negligible). The anisotropies found for **1** are much larger than those observed for any site of M^N, suggesting, again, that the assumption of six ferrous "trigonal" sites may need some modification.

Our analysis shows that B^1 represents two iron sites, and since only one ENDOR species is observed for B^1, the two sites must be equivalent. In mixed-valence clusters, equivalent magnetic sites often belong to valence-delocalized $Fe^{2+}Fe^{3+}$ pairs, and we wonder whether B^2 represents such a pair. Delocalized Fe^{2+}-Fe^{3+} pairs exhibit generally **A**-tensors with smaller anisotropies than ferrous sites, primarily because the isotropic **A**-tensor of the high-spin ferric site is averaged with the anisotropic **A**-tensor of the ferrous site.[44,45] Valence delocalization can be complete, leading to identical spectra for both sites with a δ value that is the arithmetic mean of the shifts of the ferric and ferrous sites. Alternatively, a pair may be partially delocalized, exhibiting two distinct Mössbauer spectra with parameters that are neither typical ferric nor ferrous but reflect an approach to the average. Two examples of mixed-valence complexes with fractional delocalization have recently been reported.[46,47] If M^N would contain, for instance, two or three valence-delocalized Fe^{2+}-Fe^{3+} pairs, the isomer shifts would be averaged toward $\delta \approx 0.4$ mm/s. The same phenomenon would yield **A**-tensors more isotropic than that observed for **1**. Which sites of M^N might be involved? If delocalization is assumed, B^1 would represent a completely delocalized pair, while A^1 and A^2 could represent a partially delocalized pair. A^3 and B^2 are unlikely to belong to the same pair because their **A**-tensor components have different signs. Of course, valence delocalization in a cluster containing seven iron sites is not necessarily restricted to pairs, and the present discussion might have to be extended to delocalization extending over more than two sites. We do not wish to suggest that the preceding discussion proves that M^N contains (formally) a (Mo^{4+}-$4Fe^{2+}$-$3Fe^{3+}$) core; however, given the limited information available from model complexes, the isomer shifts and anisotropies of the magnetic hyperfine tensors are better rationalized with a model comprising three Fe^{3+} rather than one Fe^{3+}.[48,49,51]

(37) Yoo, S. J.; Meyer, J.; Hendrich, M. P.; Peterson, J.; Achim, C.; Münck, E. *J. Biol. Inorg. Chem.*, in press.

(38) Moura, I.; Huynh, B. H.; Hausinger, R. P.; LeGall, J.; Xavier, A. V.; Münck, E. *J. Biol. Chem.* **1980**, *255*, 2493−2498.

(39) (a) Mascharak, P. K.; Papaefthymiou, G. C.; Frankel, R. B.; Holm R. H. *J. Am. Chem. Soc.* **1981**, *103*, 6110−6116. (b) Lane, R. W.; Ibers, J. A.; Frankel, R. B.; Papaefthymiou, G. C.; Holm, R. H. *J. Am. Chem. Soc.* **1977**, *99*, 84−98. (c) Frankel, R. B.; Papaefthymiou, G. C.; Lane, R. W.; Holm R. H. *J. Phys. C6* **1976**, *37*, 165−170.

(40) (a) Dunham, W. R.; Bearden, A. J.; Salmeen, L. T.; Palmer, G.; Sands, R. H.; Orme-Johnson, W. H.; Beinert, H. *Biochim. Biophys. Acta* **1971**, *253*, 134−152. (b) Palmer, G.; Dunham, W. R.; Fee, J. A.; Sands, R. H.; Iizuka, T.; Yonetani, T. *Biochim. Biophys. Acta* **1971**, *245*, 201−207. (c) Anderson, R. E.; Dunham, W. R.; Sands, R. H.; Bearden, A. J.; Crespi, H. L. *Biochim. Biophys. Acta* **1975**, *408*, 306−318.

(41) Comparison of the δ values with those of the $Fe^{3+}Fe^{3+}$ pair of oxidized high-potential iron proteins is not appropriate because the pair acquires electron density from the adjacent $Fe^{2+}Fe^{3+}$ delocalized pair.[22]

(42) Mouesca, J.-M.; Noodleman, L.; Case, D. A.; Lamotte, B. *Inorg. Chem.* **1995**, *34*, 4347−4357.

(43) Sanakis, Y.; Power, P. P.; Münck, E., manuscript in preparation.

(44) Achim, C.; Bominaar, E. L.; Meyer, J.; Peterson, J.; Münck, E. *J. Am. Chem. Soc.* **1999**, *121*, 3704−3714.

(45) Gamelin, D. R.; Bominaar, E. L.; Kirk, M. L.; Wieghardt, K.; Solomon, E. I. *J. Am. Chem. Soc.* **1996**, *118*, 8085−8097.

(46) Ding, X.-Q.; Bill, E.; Trautwein, A. X.; Winkler, H.; Kostikas, A.; Papaefthymiou, V.; Simopoulos, A.; Bradwood, P. Gibson, J. *J. Chem. Phys.* **1993**, *99*, 6421−6428.

(47) Hagadorn, J. R.; Prisecaru, I.; Münck, E.; Que, L.; Tolman, W. B. *J. Am. Chem. Soc.* **1999**, *121*, 9760−9761.

(48) That the molybdenum has no special effect on the isomer shifts of the M-center is indicated by the work of Huynh and co-workers, who have reported that the M-center of the *A. vinelandii* VFe protein has the same δ_{av} as the M-center of the MoFe protein.[49] Moreover, the FeFe-cofactor of an iron-only nitrogenase has a δ_{av} value that is essentially the same as that of the M-center of MoFe protein.[50]

(49) Ravi, N.; Moore, V.; Lloyd, S. G.; Hales, B. J.; Huynh, B. H. *J. Biol. Chem.* **1994**, *269*, 20920−20924.

(50) Trautwein, A. X., personal communication. Krahn, E.; Weiss, B. J. R.; Kroeckel, M.; Groppe, J.; Henkel, G.; Cramer, S. P.; Trautwein, A. X.; Schneider, K.; Mueller, A. *J. Biol. Inorg. Chem.*, submitted.

(51) Counterion chromatography,[52] DEAE binding studies,[53] and electrophoretic measurements[54] have shown that extracted cofactor is negatively charged. If three negative charges are assigned to homocitrate and if one assumes that a negatively charged ion replaces the thiolate sulfur of αCys 275, the extracted cofactor will be negatively charged in the $S = {}^3/_2$ state regardless of whether six or four Fe sites are ferrous.

Very little is known about the exchange couplings between the iron sites of the M-center. If the molybdenum site were indeed diamagnetic, or nearly so as indicated by ENDOR, the coupling problem would involve seven spins. Without some simplifications one faces the daunting task of finding the correct $S = {}^3/_2$ multiplet among the many possibilities. In attempting to solve the spin-coupling problem one would be inclined to consider, as a first approximation, the case where intracube coupling is weak compared to the coupling within the [Mo-3Fe-3S] and [4Fe-3S] subassemblies. This would allow one to construct the $S = {}^3/_2$ ground multiplet by coupling the two spins of the subcubanes. Recent studies of the double-cubane $[Fe_8S_{12}(Bu^tNC)_{12}]$ assembly show that exchange couplings involving a single sulfide bridge can be formidable ($J \approx 450$ cm^{-1}, $H = J\mathbf{S}_1\cdot\mathbf{S}_2$, Fe−Fe distance 3.28 Å).[55] While the quoted J value pertains to the coupling between two *ferric* sites, a recent study of the diferrous [2Fe-2S] ferredoxin from *Aquifex aeolicus* shows that the coupling between two ferrous sites can be formidable as well, namely $J > 80$ cm^{-1}.[23] Given the short intracubane Fe−Fe distances of the cofactor cluster (2.55 Å reported for *Av*1[9] and 2.62 Å for *Kp*1[11]), the approximation of weak intracube coupling may not be realistic.

Cluster State M^R. It is currently not proven that samples prepared under turnover conditions are homogeneous in the sense that they contain no species other than M^N and M^R, although we have no evidence for heterogeneities. To address this question one has to study samples prepared with different ratios of Fe protein to MoFe protein quenched at different times during turnover and assess whether the spectra of such samples are superpositions of M^R and M^N or whether other species are involved; such studies are in preparation.[56]

As pointed out in the Results section, the change in δ_{av} between M^N and M^R is smaller (0.02 mm/s) than the corresponding change between M^{OX} and M^N (0.06 mm/s). A change in δ_{av} of 0.06 mm/s suggests that one electron is transferred into an iron-based orbital.[57] This assessment agrees with the conclusions of Hodgson and co-workers, who suggested on the basis of XANES studies that the oxidation state of the molybdenum remains unchanged between M^{OX} and M^N.[58] The small change in δ_{av} observed after the reduction of M^N would indicate that the reduction to M^R is centered on the molybdenum. This conclusion becomes more compelling when the magnetic hyperfine interactions are taken into account.

The high-field Mössbauer spectra of M^R are strikingly similar to those of M^N (Figure 7B,C). This observation suggests that the seven iron sites display similar magnetic hyperfine interactions under conditions (i.e., at 4.2 K in strong applied fields) where the expectation value of the electronic spin is close to its saturation value. The high-field spectra of M^R and M^N are similar but not identical (because the iron sites of M^N and M^R have different ΔE_Q values, as can be seen in Figure 6B, the spectra cannot be identical under any experimental conditions). The high-field spectra of M^R indicate the presence of three *B*-sites just like the spectra of M^N, and at fields above 4.0 T, the *B*-sites in both cluster states produce nearly the same hyperfine fields. A similar observation applies to the *A*-sites, although there are some differences around +2.0 mm/s Doppler velocity. These differences could conceivably result from a site that has undergone a substantial change in ΔE_Q between the two cluster states; for instance, the shoulder at ≈1.3 mm/s in the spectrum of Figure 6B is the high-energy line belonging to a site with substantially increased ΔE_Q.

To rationalize the similar magnetic hyperfine patterns observed for M^N and M^R, we offer the following considerations. Suppose that the extra electron of M^R is accommodated in an orbital that is centered by and large on the molybdenum. ENDOR studies by Hoffman and collaborators have led to the suggestion that the molybdenum of M^N is in the 4+ ($S = 0$) state.[32] Hodgson and co-workers have reached the same conclusion on the basis of X-ray edge and near-edge absorption spectroscopy (XANES).[58] If we adopt these conclusions, reduction of the molybdenum will result in a Mo^{3+}. (We will assume, for simplicity, that the Mo^{3+} is low-spin as the Mo^{4+} of M^N; at the present level of information it is not critical whether the Mo^{3+} has spin ${}^1/_2$ or ${}^3/_2$; see ref 63). A Mo^{3+} site is paramagnetic and will have exchange interactions with the Fe5, Fe6, and Fe7,

$$H_{exch} = \sum J_i \mathbf{S}_i\cdot\mathbf{S}_{Mo} \qquad (3)$$

where i sums over iron sites 5, 6, and 7 of Chart 1. If the J couplings between the Mo and these three Fe sites are weak compared to the couplings between the seven Fe sites, we can employ the Wigner−Eckart theorem and replace the site spins $\mathbf{S}_i$ in the above expression by the spin $\mathbf{S}_{S=3/2}$ of the iron core, yielding $H_{exch} = J_{eff}\mathbf{S}_{S=3/2}\cdot\mathbf{S}_{Mo}$. We can then construct the cluster spin of the M^R ground state by coupling $\mathbf{S}_{Mo}$ of the Mo^{3+} to $\mathbf{S}_{S=3/2}$, $\mathbf{S} = \mathbf{S}_{Mo} + \mathbf{S}_{S=3/2}$. Parallel coupling between $\mathbf{S}_{Mo}$ and $\mathbf{S}_{S=3/2}$ yields an $S = 2$ ground state. If one analyzes in this model the data of M^R with an $S = 2$ spin Hamiltonian, one has to multiply all A values of Table 1 by a factor ${}^3/_4$, $\mathbf{A}_{S=2} = {}^3/_4\mathbf{A}_{S=3/2}$, and the zero-field splitting parameter becomes $D_{S=2} = D_{S=3/2}/2$[59] (see Table 3.3 of Bencini and Gatteschi[60]). Figure 8 shows a comparison of the expectation values of the electronic spin, $\langle S_i\rangle$ ($i = x,y,z$), for the lowest spin level of the $S = {}^3/_2$ system of M^N and an assumed $S = 2$ system of M^R; because the $M_S = \pm {}^1/_2$ ground state of M^N is essentially axial ($E/D = 0.05$), we have plotted the curves for $E/D = 0$. It can be seen that the two spin systems behave very differently at low field: the spin expectation values of the Kramers system of M^N start at finite values, $\langle S_i\rangle = -g_i/4$, and reach $\langle S_x\rangle = \langle S_y\rangle = -1.40$ at 8.0 T. In contrast, the non-Kramers system of M^R has $\langle S_i\rangle = 0$ in zero field (thus yielding quadrupole doublets in the spectra of Figure

(52) Huang, H. Q.; Kofford, M.; Simpson, F. B.; Watt, G. D. *J. Inorg. Biochem.* **1993**, *218*, 59−75.

(53) Wink, D. A.; McLean, P. A.; Hickman, A. B.; Orme-Johnson, W.; *Biochemistry* **1989**, *28*, 9407−9412.

(54) Yang, S.-S.; Pan, W.-H.; Friesen, G. D.; Burgess, B. K.; Corbin, J. L.; Stiefel, E. I.; Newton, W. E. *J. Biol. Chem.* **1982**, *257*, 8042−8048.

(55) Goh, C.; Nivorozhkin, A.; Yoo, S. J.; Bominaar, E. L.; Münck, E.; Holm R. H. *Inorg. Chem.* **1998**, *37*, 2926−2932.

(56) Lowe and Thorneley have analyzed *Klebsiella pneumoniae* nitrogenase in terms of a kinetic scheme that describes different oxidation states of the MoFe protein that are expected to be present during turnover under a variety of conditions.[1] The states E1−E7 represent MoFe protein molecules that have received 1−7 electrons from the Fe protein. Where those electrons reside on the MoFe protein (FeMoco, P-clusters, substrate reduction intermediates) is not treated by the scheme. Under our conditions, David Lowe has calculated that, according to the scheme, 40% of the MoFe protein should be in the $S = {}^3/_2$ state (*E*0), which is what we observe. Those calculations predict that 40% should be in the one-electron-reduced (*E*1 or M^R) state and that 20% will be split among more reduced states of the MoFe protein. Our analysis suggests that ca. 60% of the FeMoco sites are one-electron reduced.

(57) The change in δ between a ferric and ferrous FeS_4 site is ca. 0.45 mm/s. Thus, an average change of 0.06 mm/s in δ_{av} spread over seven iron sites corresponds to a change of 0.42 mm/s, i.e., roughly to about one electron.

(58) Liu, H. I.; Filipponi, A.; Gavini, N.; Burgess, B. K.; Hedman, B.; DiCicco, A.; Natoli, C. R.; Hodgson, K. O. *J. Am. Chem. Soc.* **1994**, *116*, 2418−2423.

(59) Because the zero-field splitting tensor can mix the resulting $S = 2$ or $S = 1$ multiplets, the last relation assumes that J_{eff} is sufficiently larger than the zero-field splittings.

(60) Bencini, A.; Gatteschi, D. In *EPR of Exchange Coupled Systems*; Springer-Verlag: Berlin, 1990.

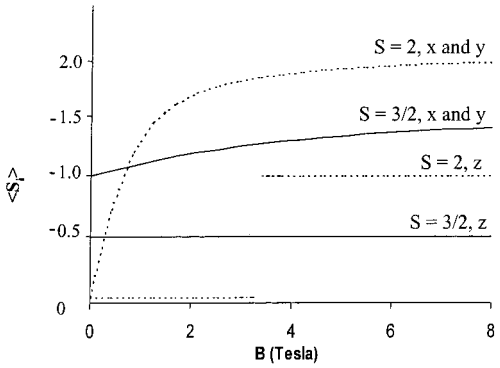

Figure 8. Expectation values of the electronic spin for the lowest level of an $S = {}^3/_2$ system ($M = -{}^1/_2$) and an $S = 2$ system ($M = 0$ level), computed for magnetic fields applied along the *x*, *y*, and *z* directions of the zero-field splitting frame. The jump for the *z* direction of the $S = {}^3/_2$ system is caused by level crossing.

6A) and attains $\langle S_x \rangle = \langle S_y \rangle = -1.94$ at 8.0 T. Thus, the internal magnetic fields along *x* and *y* are $B_{x,y}(i) = 1.40A_{x,y}(i)/g_n\beta_n$ for M^N and $B_{x,y}(i) = 1.94({}^3/_4)A_{x,y}/g_n\beta = 1.45A_{x,y}(i)/g_n\beta_n$ for M^R, suggesting that the magnetic splittings for M^N and M^R are essentially the same, as observed in the high-field spectra of Figure 7B,C. If we assume, on the other hand, that M^R has an $S = 1$ ground state, we would expect that M^R exhibits internal fields at 8.0 T that are 25% smaller than those of M^N. Finally, if the spin system of M^R has a zero-field splitting with an E/D value similar to that of M^N, we would not expect to observe an integer-spin EPR signal because possible transitions are essentially forbidden for $E/D \approx 0.05$. Indeed, parallel mode EPR studies at X- and Q-band (not shown) have not revealed any resonance attributable to M^R.

The model just outlined[63] is based on the idea that the electron added to the M-center in the transition $M^N \rightarrow M^R$ is accommodated essentially at the molybdenum site. This notion is supported by our preliminary radiolytic reduction experiments of M^N. Thus, the isomer shift change between M^N and M^I is nearly twice as large as the change between M^N and M^R and comparable to the change between M^{OX} and M^N, suggesting that the added electron of M^I has been allocated to iron sites.[61] A different allocation of the added electron is also indicated by the different magnetic hyperfine interactions observed for the two reduced states of the M-center. The similarity of the magnetic hyperfine patterns observed for M^N and M^R suggests that the arrangement of the site spins in the 7-Fe segment of the cofactor is essentially the same in both cluster states. It is unlikely that such similarities would arise if the electron that enters the cofactor in the $M^N \rightarrow M^R$ transition would be accommodated at an iron site; this would change at least one site spin and thus would modify the spin-coupling scheme. We stress that the success of the simple model outlined above, at the present level of analysis, does not quite prove our point. Clearly, more research is necessary to test the above suggestion. It should be possible to determine the spin of M^R by measuring the magnetic susceptibility and Mössbauer spectra of the same sample, although such measurements are by no means straightforward.

We have suggested here that the isomer shifts and *A* values of M^N are better rationalized by assuming that M^N has a (Mo^{4+}-$3Fe^{3+}$-$4Fe^{2+}$-$9S^{2-}$) core. This assessment is based on the δ and *A* values of one mononuclear complex, **1**, with a trigonal sulfur coordination. The X-ray structures of the MoFe protein indicate short Fe−Fe distances for six irons of the M-center, although the metric data differ for the *Av*1 (2.55 Å average Fe−Fe distance at 2.0 Å resolution) and *Kp*1 (2.62 Å at 1.6 Å resolution) structures. Above we have suggested that the core of M^N contains (formally) $3Fe^{3+}$, $4Fe^{2+}$, and one Mo^{4+} and that reduction of M^R involves the molybdenum in a substantial way (but not exclusively, as indicated by the increase in δ in going from M^N to M^R). We wish to stress that the assessment of the oxidation state of the iron components of M^N rests on the assumption that the six "trigonal" Fe sites are high-spin with properties modeled by the only available synthetic complex, namely the Power complex **1**. However, the cofactor has unique structural features, and, therefore, the synthesis of suitable model complexes should remain a high priority in nitrogenase research.

Conclusions

The present study of $^{57}M^{56}P$ hybrids of the MoFe protein has yielded the following principal results:

(1) We have identified the seventh Fe site, A^4, of the M-center that has eluded previous identification by Mössbauer and ENDOR spectroscopies. The **A**-tensor components of this site are much smaller than those of the other sites (Table 1), suggesting that the local spin of A^4 is oriented nearly perpendicular to the direction of the system spin, a situation similar to that found in the $S = {}^1/_2$ state of [3Fe-4S] clusters.[31]

(2) Our analysis shows that M^N has three *B*-sites and that B^1 represents two Fe sites. Because only two *B*-type **A**-tensors were observed with ENDOR over the whole range of molecular orientations, our result implies the presence of two strictly equivalent *B*-sites.

(3) Analyses of ENDOR[32] and XANES[58] data of the $S = {}^3/_2$ state of the M-center have led to the conclusion that the molybdenum is in the 4+ state. Comparison of the average isomer shifts of M^N with that of the only available Fe^{2+} complex with trigonal sulfur coordination suggests to us that the core of M^N is perhaps better described as (Mo^{4+}-$3Fe^{3+}$-$4Fe^{2+}$) rather than (Mo^{4+}-Fe^{3+}-$6Fe^{2+}$).

(4) The change in δ_{av} between M^{OX} and M^N suggests that the redox event is centered on the iron components of the cofactor, a conclusion reached also from the analysis of XANES[58] data. The substantially smaller change in δ_{av} between M^N and M^R indicates that the molybdenum becomes reduced in the transition to M^R. This conclusion is supported by consideration of the similarity between the magnetic hyperfine interactions observed for M^R and M^N. The model considered here requires that the exchange interactions between a Mo^{3+} of M^R and the three adjacent Fe sites be smaller than the couplings among the Fe-sites.

(5) Finally, in a preliminary study we have produced, by irradiation of ($^{57}M^{56}P$) MoFe protein with synchrotron X-rays, a new one-electron reduced state of the M-center, called M^I. M^I exhibits a larger δ_{av} value than M^R, suggesting that the reduction is centered on the iron components of the M-center.

(61) The observation that M^R and M^I have different electronic structures suggests that the M-center is in a different conformation in both states. The reader should keep in mind that M^R is quenched under turnover conditions in the presence of Fe protein, substrate, and MgATP and that M^I is obtained by reduction of M^N at 77 K. Moreover, because electrochemically reduced cofactor[18] has not been characterized spectroscopically, it is not clear how M^R or M^I is related to reduced FeMo cofactor.

(62) Musgrave, K. B.; Angove, H. C.; Burgess, B. K.; Hedman, B.; Hodgson, K. O. *J. Am. Chem. Soc.* **1998**, *120*, 5325−5326.

(63) If we assume that M^R contains a Mo^{3+} with $S_{Mo} = {}^3/_2$ and couple both systems to $S = 3$, the Mössbauer spectra in strong applied fields would be very similar to the case discussed in the text; thus, at saturation the internal fields for both cases will be $B_{int} = -({}^3/_2)A_{S=3/2}/g_N\beta_N$. In weak applied fields, e.g., at $B < 1.0$ T (for which the spectra are poorly resolved), the magnetization curves, $\langle S_l \rangle$ vs *B*, would have slopes that depend critically on the (unknown) zero-field splitting of the Mo^{3+}.

Acknowledgment. We thank Dennis R. Dean and Jason H. Christiansen for providing the FeMoco-deficient His-tagged MoFe protein strain and for help with its purification. This work is partially based upon research conducted at the Cornell High Energy Synchrotron Source (CHESS) which is supported by the National Science Foundation under award DMR 97-13424. We are grateful for the efforts of Timothy Elgren (Hamilton College) and Ernie Fontes (CHESS) for the sample irradiation. We also thank David Lowe for calculations using the Lowe−Thorneley scheme. This research was supported by National Science Foundation Grant MCD-9416224 (E.M.) and National Institutes of Health Grant GM-45209 (B.K.B).

Note Added in Proof

While reviewing the galley proof we recognized that we had used a proportional counter with a beryllium window that contained an iron contaminant. This contaminant produces a single absorption line at ≈0.3 mm/s with 0.25% amplitude. It contributes ca. 1.5% of the total absorption in our high-field spectra. This contaminant is readily recognized in the difference spectrum of Figure 5B, where it produced a mismatch between the theory and the data. Removing the contaminant and refitting the spectra yielded parameters essentially identical to those quoted in the manuscript.

JA000254K